

# Repeated Whole-Genome Duplication, Karyotype Reshuffling, and Biased Retention of Stress-Responding Genes in Buckler Mustard

Céline Geiser,<sup>a</sup> Terezie Mandáková,<sup>b</sup> Nils Arrigo,<sup>c</sup> Martin A. Lysak,<sup>b</sup> and Christian Parisod<sup>a,1</sup>

<sup>a</sup>Laboratory of Evolutionary Botany, University of Neuchâtel, 2000 Neuchâtel, Switzerland

<sup>b</sup>Plant Cytogenomics Research Group, Central European Institute of Technology, Masaryk University, Brno 625 00, Czech Republic

<sup>c</sup>Department of Ecology and Evolution, University of Lausanne, 1015 Lausanne, Switzerland

ORCID IDs: 0000-0003-0318-4194 (M.A.L.); 0000-0001-8798-0897 (C.P.)

**Whole-genome duplication (WGD) is usually followed by gene loss and karyotype repatterning. Despite evidence of new adaptive traits associated with WGD, the underpinnings and evolutionary significance of such genome fractionation remain elusive. Here, we use Buckler mustard (*Biscutella laevigata*) to infer processes that have driven the retention of duplicated genes after recurrent WGDs. In addition to the  $\beta$ - and  $\alpha$ -WGD events shared by all Brassicaceae, cytogenetic and transcriptome analyses revealed two younger WGD events that occurred at times of environmental changes in the clade of Buckler mustard (*Biscutelleae*): a mesopolyploidy event from the late Miocene that was followed by considerable karyotype reshuffling and chromosome number reduction and a neopolyploidy event during the Pleistocene. Although a considerable number of the older duplicates presented signatures of retention under positive selection, the majority of retained duplicates arising from the younger mesopolyploidy WGD event matched predictions of the gene balance hypothesis and showed evidence of strong purifying selection as well as enrichment in gene categories responding to abiotic stressors. Retention of large stretches of chromosomes for both genomic copies supported the hypothesis that cycles of WGD and biased fractionation shaped the genome of this stress-tolerant polyploid, promoting the adaptive recruitment of stress-responding genes in the face of environmental challenges.**

## INTRODUCTION

Multiple rounds of whole-genome duplication (WGD) have shaped genome evolution throughout eukaryotes (Lynch and Conery, 2000; Wolfe, 2001; Van de Peer et al., 2009). In particular, WGDs have greatly contributed to plant evolution and speciation (Wood et al., 2009; Jiao et al., 2011). However, to what extent WGD leads to the origin of novel adaptive traits and fosters species radiation remains controversial (Ohno, 1970; Arrigo and Barker, 2012; Soltis et al., 2014). Comprehensive understanding of the molecular and evolutionary processes underlying the preservation and diversification of duplicated genes may thus be central to an integrative consideration of organismal diversity (McGrath and Lynch, 2012; Nei, 2013).

The importance of WGD as a major source of variation has been increasingly recognized with the documentation of various molecular mechanisms operating to restore structurally and functionally diploid states within a few million years (i.e., diploidization; Lim et al., 2007; Doyle et al., 2008; Freeling, 2009; Mandáková et al., 2010; Tayalé and Parisod, 2013). However, numerous duplicated genes escape deletion or other forms of pseudogenization (i.e., a phenomenon collectively referred as fractionation) and are stably retained over the long term (Freeling et al., 2012).

Such retained duplicates contribute greatly to the genomes of paleopolyploids or younger mesopolyploids, and several non-mutually exclusive models have been proposed to account for their maintenance after WGD (Flagel and Wendel, 2009; Innan and Kondrashov, 2010). In particular, the overarching gene balance hypothesis posits that alteration of the stoichiometry among interacting gene products is detrimental, fostering stable transmission of duplicates through purifying selection (Birchler and Veitia, 2012). Such a central role of gene dosage may explain the preferential retention of highly expressed genes following WGD (Garsmeur et al., 2014; Woodhouse et al., 2014). On the other hand, hypotheses related to change of function assume that one of the duplicated genes explores innovative functions (i.e., neo- or subfunctionalization leading to new or partitioned tasks) through neutral processes and positive selection (McGrath and Lynch, 2012). Various mechanisms certainly support the long-term retention of duplicates, but no consensus has yet emerged and their impact on species diversification remains elusive.

Analysis of plant genomes provided evidence of independent WGD events close to the Cretaceous-Paleogene boundary, supporting the origin of several paleopolyploids during the major extinction crisis that occurred approximately 65 million years ago (MYA; Fawcett et al., 2009; Vanneste et al., 2014b). The  $\beta$ -WGD event preceding the diversification of core Brassicales was postulated to be a result of this burst of polyploidy, but a recent study on this clade estimated this WGD to have occurred 90 MYA (Edger et al., 2015). The radiation of all Brassicaceae clades took place after a subsequent  $\alpha$ -WGD event that is congruently dated around 30 MYA by independent studies (Edger et al., 2015;

<sup>1</sup> Address correspondence to christian.parisod@unine.ch.

The author responsible for distribution of materials integral to the findings presented in this article in accordance with the policy described in the Instructions for Authors (www.plantcell.org) is: Christian Parisod (christian.parisod@unine.ch).

www.plantcell.org/cgi/doi/10.1105/tpc.15.00791

Hohmann et al., 2015). In addition to these multiple rounds of WGD having shaped the paleopolyploid crucifer genomes, transcriptome analysis in 23 Brassicaceae species recently revealed the origin of several mesopolyploids during the late Miocene (i.e., 10 to 5 MYA; Kagale et al., 2014). Despite apparently nonrandom distribution of WGD in time, the mechanisms promoting the radiation of polyploids remain poorly understood (Parisod et al., 2010; Vanneste et al., 2014a).

The genus *Biscutella* (Brassicaceae) comprises ~50 species covering the whole Mediterranean basin and is mostly diversified in Southwestern Europe (Jalas et al., 1996). It apparently diverged relatively early from other Brassicaceae (Couvreur et al., 2010) and shows remarkable genomic variation, comprising species with chromosome numbers of either  $x = 6$ ,  $x = 8$ , or  $x = 9$  (Olowokudejo, 1986). Only specific taxa with  $x = 9$  extended northward of the Mediterranean area and reached high elevation in central Europe. Accordingly, the Buckler mustard species complex (*Biscutella laevigata*) was postulated as case study of alpine taxon having colonized the Alps in relation with autopolyploidy (i.e., WGD; Schönfelder, 1968; Favarger, 1971). This taxon indeed currently occurs as diploid populations ( $2n = 2x = 18$ ) in thermophilous habitats of never-glaciated areas of central Europe, whereas multiple autotetraploid lineages ( $2n = 4x = 36$ ) have established in a wide range of alpine habitats during the glacial cycles of the late Quaternary (Manton, 1937; Tremetsberger et al., 2002; Parisod and Besnard, 2007). Here, we use comparative chromosome painting in diploids and transcriptomics in autopolyploids of the Buckler mustard species to infer recurrent WGD events. Biased fractionation resulted in the retention of duplicates that show evidence of selection and that are preferentially involved in responses to ecological stressors. How genetic and environmental constraints may interact during WGD fractionation cycles and shape genomes is discussed.

## RESULTS

### Karyotype of Buckler Mustard

Chromosome painting in diploid Buckler mustard (*B. laevigata* subsp *varia*,  $2n = 2x = 18$ ) revealed a diploid-like karyotype, with nine bivalents in diakinesis and metaphase I (Figure 1). In addition to distinct domains of pericentromeric heterochromatin, two interstitial heterochromatic knobs were detected on the bottom arm of chromosome Bv2. Two chromosome pairs bear terminal 35S rDNA (Bv2 and Bv3), whereas 5S rDNA loci were observed in the pericentromeric region on three chromosomes (Bv1, Bv4, and Bv9). Given the lack of genetic map, the ancestral crucifer karyotype (ACK) with 24 genomic blocks (GBs) on eight chromosomes (AK1-8; Schranz et al., 2006) served as a reference for the construction of the *B. laevigata* karyotype using comparative chromosome painting (CCP; Figure 1). Although six copies of the shortest GBs (G2, H2, part of I1 = I1a, S1, T1, and T2) could not be placed into the map, all the remaining GBs (87.5%) were found duplicated. Homoeologous *Arabidopsis thaliana* BAC contigs indeed hybridized to two different chromosomes within haploid pachytene complements of diploid *Biscutella* (only both copies of GB J hybridized to the same chromosome). The GB duplicates

slightly but consistently differed in length and fluorescence intensity; the longer and brighter copy was labeled as #1 (Figure 1).

Several ancestral GB associations matching the ACK with eight chromosomes have been detected in the *Biscutella* karyotype. The characteristic GB association D/E of ancestral chromosome AK2 was located on chromosomes Bv3 and Bv9, whereas AK1-derived blocks A and B (and C) were together on Bv4 and Bv7. Similar to the ancestral chromosome AK4, genomic copies of J (J#1 and #2) as well as a part of I (I#1b) were on chromosome Bv6, whereas AK3-derived GBs F/G/H were together on Bv8. In contrast, chromosomes Bv5 and Bv6 possessed the O/P/W/R association that is diagnostic for ACK-derived proto-Calepineae karyotype (PCK) with  $n = 7$  (Mandáková and Lysak, 2008). The origin of chromosome Bv6 apparently involved two centromere inactivation/deletion events preserving the collinearity of ancestral chromosomes PCK4 (AK4) and PCK6 (AK6/8). Furthermore, Bv1 and Bv4 presented PCK-like association of blocks Q and X. These O/P/W/R and Q/X block combinations thus link the ancestral *Biscutella* genome to an eight-chromosome precursor of PCK (Supplemental Figure 1).

### Inference of WGDs with Transcriptomics

Genome dynamics involving WGD fractionation cycles were confirmed by the analysis of the Buckler mustard transcriptome that was iteratively assembled from long 454 reads and short SOLiD reads from leaf and root tissues of *B. laevigata* subsp *laevigata* ( $2n = 4x = 36$ ; the autopolyploid relative of *B. laevigata* subsp *varia*; Supplemental Tables 1 and 2). After removal of perfectly duplicated contigs as well as contigs smaller than 150 bp, the transcriptome yielded 102,998 contigs (mean length, 413.50 bp; N50, 573 bp; for a total of 42,589,854 bp). BLASTx against the TAIR10 peptide database revealed 72,273 (70.1%) and 64,645 (62.7%) contigs annotated at e-values of  $e^{-5}$  and  $e^{-10}$ , respectively. These contigs represented 16,389 unigenes (49% of genes in *Arabidopsis*) distributed among all GBs (Supplemental Figure 2), highlighting the representativeness and high quality of the inferred transcriptome. Genic contigs were translated into their reading frame, yielding 57,783 valid ESTs (thereafter called transcripts), among which 26,815 were grouped into 3141 families with at least two members. PAML estimated divergence between pairs of transcripts in each family for both nonsynonymous ( $K_a$ ) and synonymous ( $K_s$ ) substitutions.

Mixture models fitted four significant normal distributions on the distribution of  $K_s$  between 20,890 pairs of transcripts larger than 450 bp showing  $K_s < 2$  (Table 1; Supplemental Figure 3), indicating large-scale gene duplications in the past of Buckler mustard. The oldest significant peak at mean  $K_s = 1.678$  likely corresponds to the  $\beta$ -WGD event specific for the core Brassicales (Bowers et al., 2003; Lysak and Koch, 2011), whereas the peak at  $K_s = 0.886$  matches the  $\alpha$ -WGD event at the basis of the Brassicaceae. Two significant peaks characteristic of the clade analyzed here were further highlighted and strongly supported: (1) a WGD event (called BI-m-WGD, referring to a mesopolyploidy event in the past of *B. laevigata*) that yielded duplicates with a mean  $K_s = 0.235$  and that was also apparent in the karyotype of diploid *B. laevigata* subsp *varia* (Figure 1) and (2) a WGD event (called BI-n-WGD, referring to a neopolyploidy event in the past of *B. laevigata*) at  $K_s = 0.032$  that

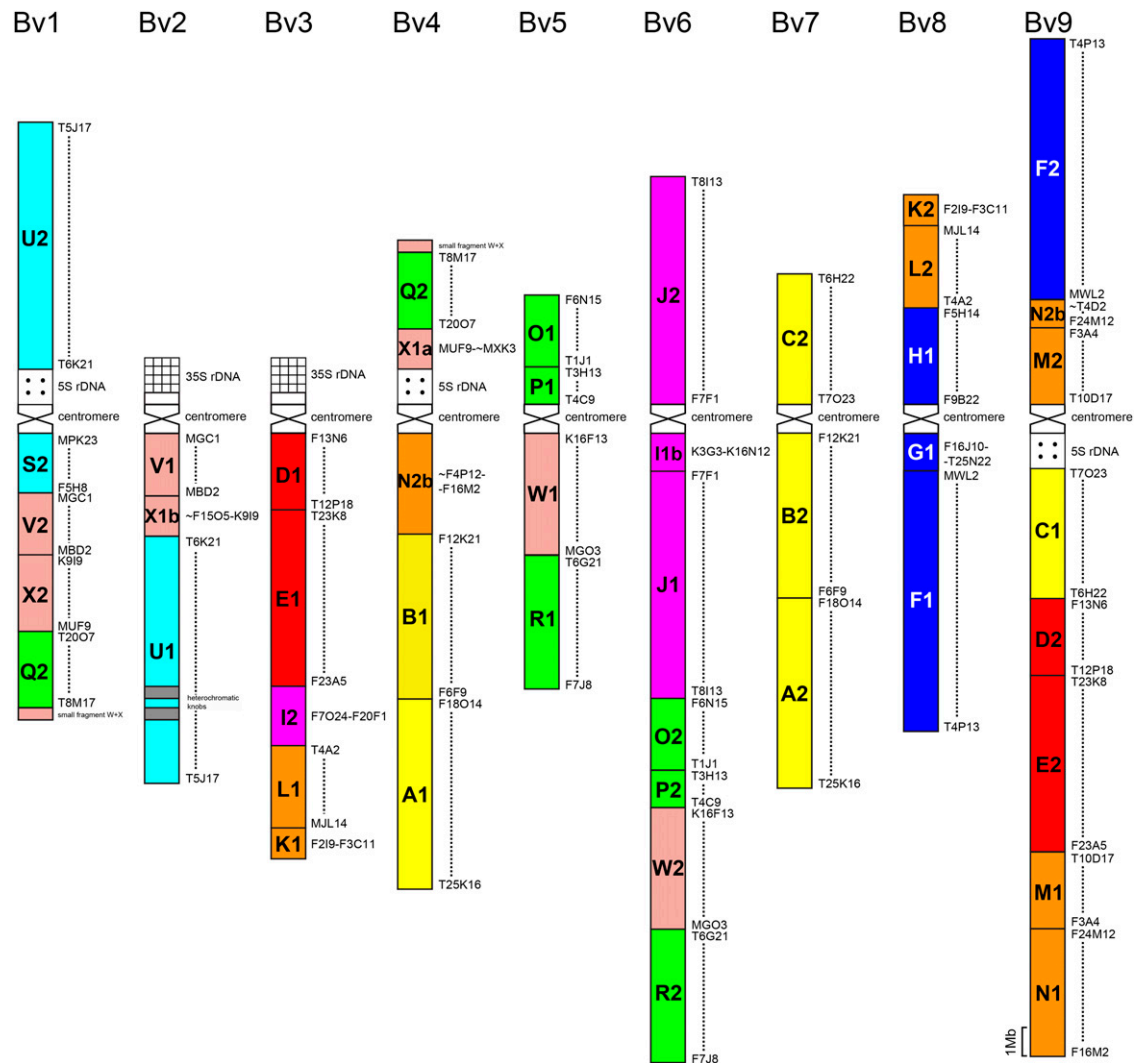


**Figure 1.** Karyotype of Buckler Mustard.

Cytomolecular comparative map of *B. laevigata* subsp *varia* ( $2n = 2x = 18$ ) based on chromosome painting analyses. Colors of 48 GBs (A to X) reflect their position on the eight chromosomes AK1 to AK8 in the ACK. The longer and more fluorescent GB duplicates are labeled as #1 and the shorter and less fluorescent copies as #2. Six GBs (G2, H2, I1a, S1, T1, and T2) cannot be localized and are not considered. The size of GBs proportionally corresponds to the size of homoeologous blocks in the *Arabidopsis* genome, as delimited by *A. thaliana* BAC clones (Supplemental Table 4).

was only apparent in the transcriptome of autotetraploid *B. laevigata* subsp *laevigata*. As a number of duplicates from this latter  $n$ -WGD event may have collapsed into consensus sequences, it was not further investigated here. Using the  $\alpha$ -WGD as calibration point (Hohmann et al., 2015), coarse dating of those WGD events pointed to  $\sim 8.6$  MYA for the BI-m-WGD event and 1.2 MYA for the BI-n-WGD event (Table 1). Such dating is consistent with evidence of mesopolyploidy events in other species (Kagale et al., 2014) and autopolyploidy in *B. laevigata* (Manton, 1937), respectively.

### Genome Restructuring and Retention of Duplicates

Both the  $\alpha$ -WGD and the BI-m-WGD events provided enough resolution to assess the evolutionary forces involved in the

retention of duplicated transcripts. The  $K_a/K_s$  ratio (i.e.,  $\omega$ ) between the 5126 pairs of transcripts having their origin after the  $\alpha$ -WGD event (i.e.,  $\alpha$ -duplicates showing  $K_s$  within the 95% confidence interval of the peak) and between the 3933 pairs from the BI-m-WGD event (i.e., BI-m-duplicates with  $K_s$  within the 95% confidence interval of the peak) highlighted most duplicates with  $\omega$  lower than 1 (Figure 2). Such depletion of nonsynonymous substitutions indicates that purifying selection is likely prevalent among retained duplicates. In contrast, only 592 pairs of  $\alpha$ -duplicates (11.5%) and 150 pairs of BI-m-duplicates (3.8%) presented evidence of positive selection with  $\omega$  higher than 1. The  $\alpha$ -WGD event thus yielded a significantly higher proportion of duplicated transcripts with evidence of positive selection than the younger BI-m-WGD event (two-sided proportion test,  $z = 12.68$ ,  $P < 0.01$ ).

**Table 1.** Mixture Model of Synonymous Substitution ( $K_s$ ) Distribution among Pairs of Transcripts Identifying Significant Peaks Indicative of WGD Events in Buckler Mustard (*B. laevigata* subsp *laevigata*;  $2n = 4x = 36$ )

WGD Event	BI-n	BI-m	$\alpha$	$\beta$
Mean $K_s \pm$ SD	$0.032 \pm 0.023$	$0.235 \pm 0.121$	$0.886 \pm 0.366$	$1.678 \pm 0.198$
Estimated age $\pm$ SD (MYA) <sup>a</sup>	$1.17 \pm 0.84$	$8.59 \pm 4.42$	32.42	$61.36 \pm 7.24$

Means and SD of  $K_s$ -based age of duplicates were computed by 100 bootstraps and used to estimate the age of WGD events.

<sup>a</sup>Calibration according to the  $\alpha$ -WGD event that occurred 32.42 MYA following Hohmann et al. (2015).

Comparative chromosome painting showed that BI-m-duplicated GBs differed slightly but consistently in their physical length and corrected total fluorescence (see Figure 3 for examples). The longer and more fluorescent copy (labeled #1) of GBs A, B, E, J, O, P, R, and U was on average 1.55 times longer and presented 1.53 times higher fluorescence than the other copy (labeled #2; Table 2), indicating preferential fractionation of one copy. Whether the same subgenome is consistently more fractionated cannot be assessed with available data and must be further evaluated through phylogenomic approaches. Assuming conservation of the gene order within BACs between *Arabidopsis* and *Biscutella*, transcripts were mapped on the karyotype to gather additional insights on the mechanisms underlying fractionation. The proportion of duplicated transcripts among GBs strongly correlated with neither the ratio of fluorescence (robust regression,  $P = 0.54$ ) nor the ratio of physical length between the longer and the shorter duplicated GB (robust regression,  $P = 0.047$ ,  $R^2 = 0.52$ ). Despite uniform density of transcripts along those GBs, retained duplicates appeared mostly as stretches of nearby loci conserved under purifying selection (Supplemental Figure 2). Duplicated chromosome segments retained along GBs A, E, and U finely colocalized with inferred sections rich in duplicated transcripts (Figure 3). Mechanisms responsible for uneven reorganization of duplicates across the genome and particularly shorter and less fluorescent regions remain elusive and must be assessed with transcriptome and genome sequencing.

### Functionally Biased Retention

Transcripts corresponding to 12,848 unigenes did not group into a family. Although transcriptome data can hardly offer conclusive evidence, they were enriched in five Gene Ontology (GO) categories (i.e., DNA recombination, DNA dependent replication, DNA repair, response to DNA damage stimulus, and DNA metabolic process; Supplemental Table 3) compared with transcripts showing evidence of retained duplicates. These functional categories show consistent restoration of single copy states in flowering plants (De Smet et al., 2013).

Using high-quality GO annotations from *Arabidopsis* as source of functional information for the related Buckler mustard, retained  $\alpha$ -duplicates and BI-m-duplicates with evidence of neutral divergence or weak selection ( $\omega$  between 0.6 and 2) showed significant overrepresentation for only a few functional categories (Figure 4). In contrast, duplicates showing evidence of strong selection were significantly enriched in particular GO categories, providing insights on the selective agents having played an important role for gene retention. Duplicates retained under strong positive selection ( $\omega$  higher than 2) after both the  $\alpha$ -WGD and the m-WGD events were related to cytoskeleton organization,

whereas duplicates showing evidence of strong purifying selection were significantly enriched in GO functions related to responses to ecological stressors. In particular, the vast majority of BI-m-duplicates retained under strong purifying selection (i.e.,  $\omega$  lower than 0.6) were chiefly enriched for GO categories related to environmental stresses, such as temperature, light, or soil chemistry (Figure 4).

## DISCUSSION

### Recurrent WGDs during Environmental Crises

Comparative chromosome painting in the Buckler mustard highlighted arrangements of GBs characteristic of both the ACK ( $n = 8$ ; Schranz et al., 2006) and the more derived PCK ( $n = 7$ ;

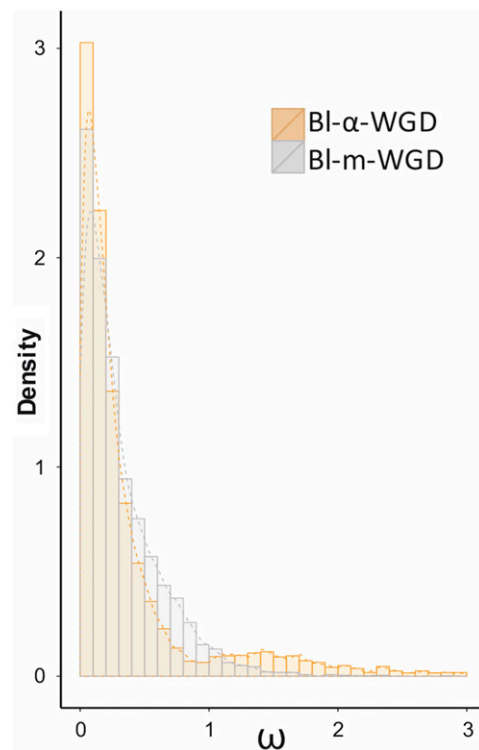


**Figure 2.** Evidence of Selection among Duplicates.

Ratio ( $\omega$ ) of nonsynonymous and synonymous substitutions between duplicated transcripts having originated at the  $\alpha$ -WGD and the BI-m-WGD events (colored according to the panel) in Buckler mustard.

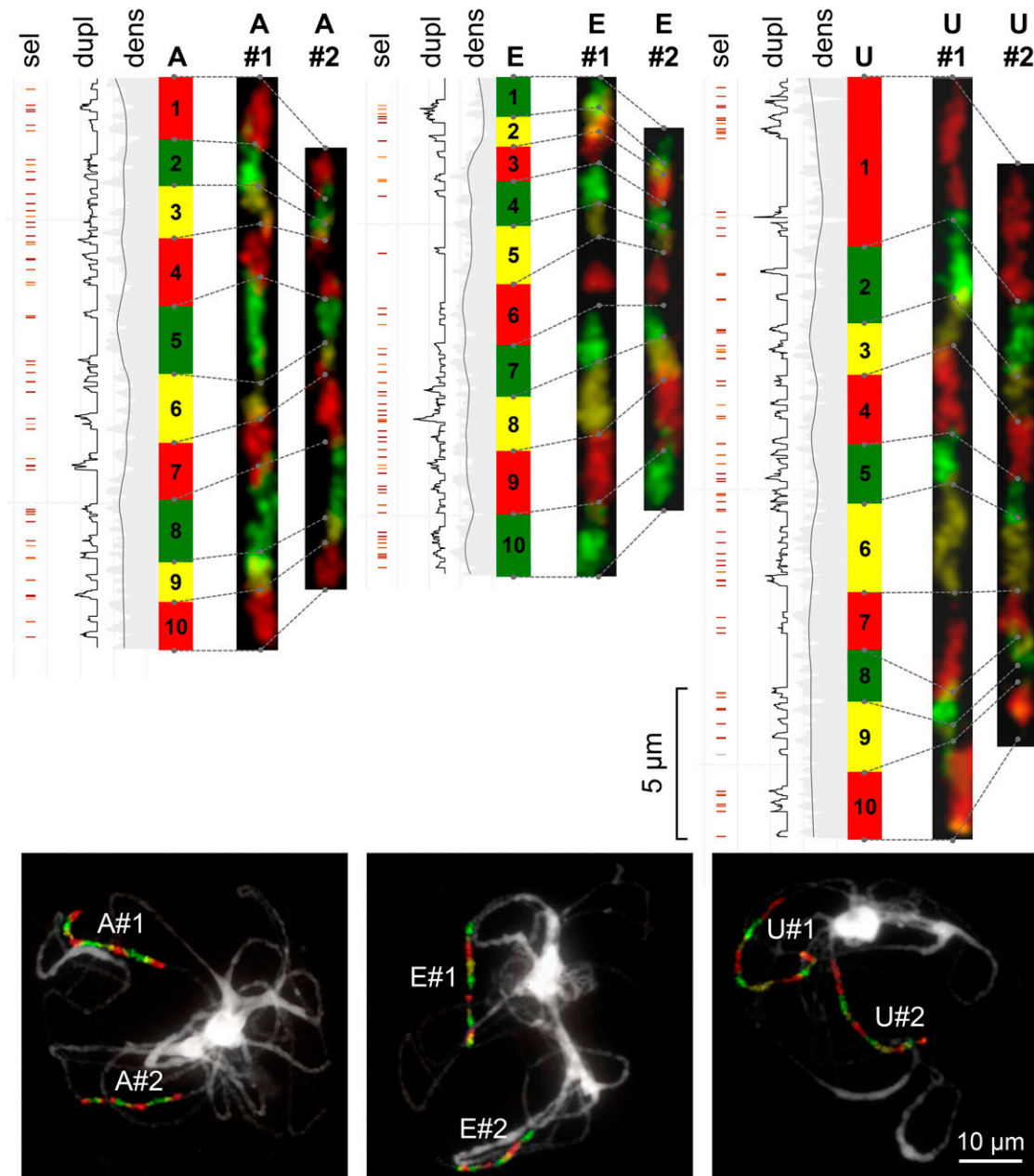


**Figure 3.** Biased Fractionation following the BI-m-WGD Event in Buckler Mustard.

Fine-scale CCP along GBs A, E, and U is associated with the distribution of retained BI-m-duplicates in the transcriptome. Transcriptome data are presented on the left of each GB, with the density of transcripts (dens) and of retained duplicates (dupl) as well as evidence of weak (light red) to strong (dark red) purifying selection (sel) along retained duplicates. Using CCP, the longest and most fluorescent GB copy was labeled as #1, and pachytene chromosomes (shown at the bottom) were straightened and displayed alongside the transcriptome data according to differentially painted sub-blocks (Supplemental Data Set 1).

Mandáková and Lysak, 2008). Presence of PCK-specific GB associations (O/P/W/R and Q/X) but absence of distinctive PCK5-like association (V/K/L/Wa/Q/X) indicate divergence of the ancestral *Biscutella* karyotype from the ACK before the establishment of the PCK genome. Phylogenetic connection of the Biscutelleae tribe to those of the extended lineage II remains to be clarified (Couvreur et al., 2010), but CCP supports early

divergence of an ancestral *Biscutella* genome with eight chromosomes. Accordingly, the BI-m-WGD event likely established a tetraploid genome with 16 chromosomes that underwent genome fractionation, with massive chromosome reshuffling and chromosome number reduction toward  $n = 9$  in *B. laevigata* and  $n = 8$  and 6 in other *Biscutella* species (Supplemental Figure 1). Future phylogenomic work will address the progenitor(s) of this

**Table 2.** Length, Corrected Total Fluorescence, and Duplicated Genes among Selected GBs in Buckler Mustard

GB	Average Length ( $\mu\text{m}$ ) <sup>a</sup>			Average CTF <sup>a</sup>			Transcriptome <sup>b</sup>		
	#1	#2	Ratio	#1	#2	Ratio	Unigenes	Duplicated Loci	Retained (%)
A	20.5	14.6	1.40	4.7E-04	3.0E-04	1.58	988	54	5.46
B	16.8	17.8	1.06	5.9E-04	3.8E-04	1.54	696	31	4.45
E	19.6	15.6	1.25	5.0E-04	3.4E-04	1.48	818	50	6.11
J	22.0	17.4	1.26	8.0E-04	3.7E-04	2.19	911	45	4.94
O	8.0	4.0	2.00	4.1E-04	3.5E-04	1.18	237	11	4.64
P	6.0	2.0	3.00	9.4E-05	1.0E-04	0.93	135	5	3.70
R	16.0	11.0	1.45	3.7E-04	1.6E-04	2.22	1116	57	5.11
U	24.8	22.0	1.13	5.8E-04	5.3E-04	1.09	1330	75	5.64

<sup>a</sup>Averaged measure from painting of multiple pachytene chromosomes, with #1 representing the longer and more fluorescent copy. CTF, corrected total fluorescence.

<sup>b</sup>Percentage retained as the proportion of unigenes in the transcriptome that were located in the corresponding GB and showed evidence of BI-m-duplicates.

mesopolyploid lineage, but we note that related genera present high chromosome numbers (e.g., *Lunaria* with  $n = 14, 15$ ; Couvreur et al., 2010), suggesting that the BI-m-WGD event may predate the diversification of the *Biscutella* genus.

The transcriptome of Buckler mustard assembled by combining advantages of short and long reads into a set of long and framed transcripts largely confirmed cytogenetic conclusions and offered additional insights on the evolutionary processes underlying WGD fractionation cycles. Consistent peaks in the distribution of  $K_s$  between duplicated transcripts highlighted four WGD events in the history of Buckler mustard. In addition to evidence matching with the well-known core Brassicales-specific  $\beta$ -WGD event and the 30 million-year-old  $\alpha$ -WGD event that predates the radiation of the Brassicaceae (Bowers et al., 2003; Lysak and Koch, 2011; Schranz et al., 2012), the  $K_s$  distribution pointed to two younger peaks (BI-m-WGD at  $K_s = 0.235$  and BI-n-WGD at  $K_s = 0.032$ ) indicative of recurrent WGD events in the more recent past of *B. laevigata*.

According to the dating of WGD events across angiosperms and Brassicaceae (Lysak and Koch, 2011; Hohmann et al., 2015), the mesopolyploidy BI-m-WGD event ( $\sim 8$  MYA) dates from the late Miocene era (5.3 to 11.6 MYA), when several other Brassicaceae species underwent WGD events (Kagale et al., 2014). This period was characterized by increasing seasonal aridity as well as major climatic changes such as the Messinian salinity crisis that strongly impacted Mediterranean vegetation (Blondel et al., 2010). It thus seems likely that environmental changes favored the BI-m-WGD event among *Biscutella* ancestors. Evidence of the BI-m-WGD event in the karyotype of the diploid *B. laevigata* subsp *varia* ( $2n = 2x = 18$ ) indicates that the latter BI-n-WGD event corresponds to the recent origin of autotetraploids *B. laevigata* subsp *laevigata* ( $2n = 4x = 36$ ) that occurred during the Pleistocene ice ages (Manton, 1937; Parisod and Besnard, 2007). The n-WGD event thus also points to a period with major environmental changes across the Buckler mustard distribution range. Although  $K_s$ -based estimates offer rough dates to be taken with caution, recurrent WGD events in Buckler mustard appear consistent with data available from other species (Kagale et al., 2014; Vanneste et al., 2014b; Hohmann et al., 2015) and support the hypothesis that ecological challenges sustain evolution through polyploidy (Parisod et al., 2010; Vanneste et al., 2014a).

Recurrent WGDs followed by chromosome repatterning and descending dysploidy leading to diploid-like chromosome numbers within a few million years, as observed here, are fully congruent with genome dynamics reported in other Brassicaceae clades (Bowers et al., 2003; Mandáková et al., 2010; Chalhoub et al., 2014). Compared with other species having undergone a WGD event at the same time and still showing polyploid chromosome numbers (Kagale et al., 2014), Buckler mustard has gone through intense karyotype reshuffling. Similarly remarkable post-WGD genome evolution was also reported in the genus *Brassica* (Chalhoub et al., 2014). However, unlike the mesopolyploid *Brassica* genomes that involved genome triplication as well as subsequent allopolyploidy (Tang et al., 2012), *B. laevigata* underwent tetraploidization and autopolyploidy, ideally complementing investigation of the processes shaping polyploid genomes.

### Biased Genome Fractionation over Time

The transcriptome of *B. laevigata* shed further light on the mechanisms underlying genome reorganization after recurrent WGDs by comparing duplicated transcripts that originated at the  $\alpha$ - and BI-m-WGD events. Pairs of transcripts analyzed here are predominantly derived from those WGD events (Supplemental Analysis) and, although specific loci may find their origin in other types of duplication, WGD appears as likely responsible for patterns observed in the genome of Buckler mustard. The  $K_a/K_s$  ratio ( $\omega$ ) highlighted that the majority of duplicates retained after both WGD events showed evidence of selection, matching predictions of biased fractionation over evolutionary times (Innan and Kondrashov, 2010; McGrath and Lynch, 2012). In particular, retained genes with evidence of positive selection ( $\omega > 1$ ) were significantly more frequent among older duplicates (i.e., retained after the  $\alpha$ -WGD) than younger ones (BI-m-WGD), matching a lag-time model whereby adaptive recruitment of innovative duplicates occurs long after their origin (Schranz et al., 2012; Tank et al., 2015). Remarkably, only duplicates related to cytoskeleton organization were retained under strong positive selection after both the  $\alpha$ - and m-WGD events. With increased cell volume being one of the few constant alterations induced by polyploidy (Ramsey and

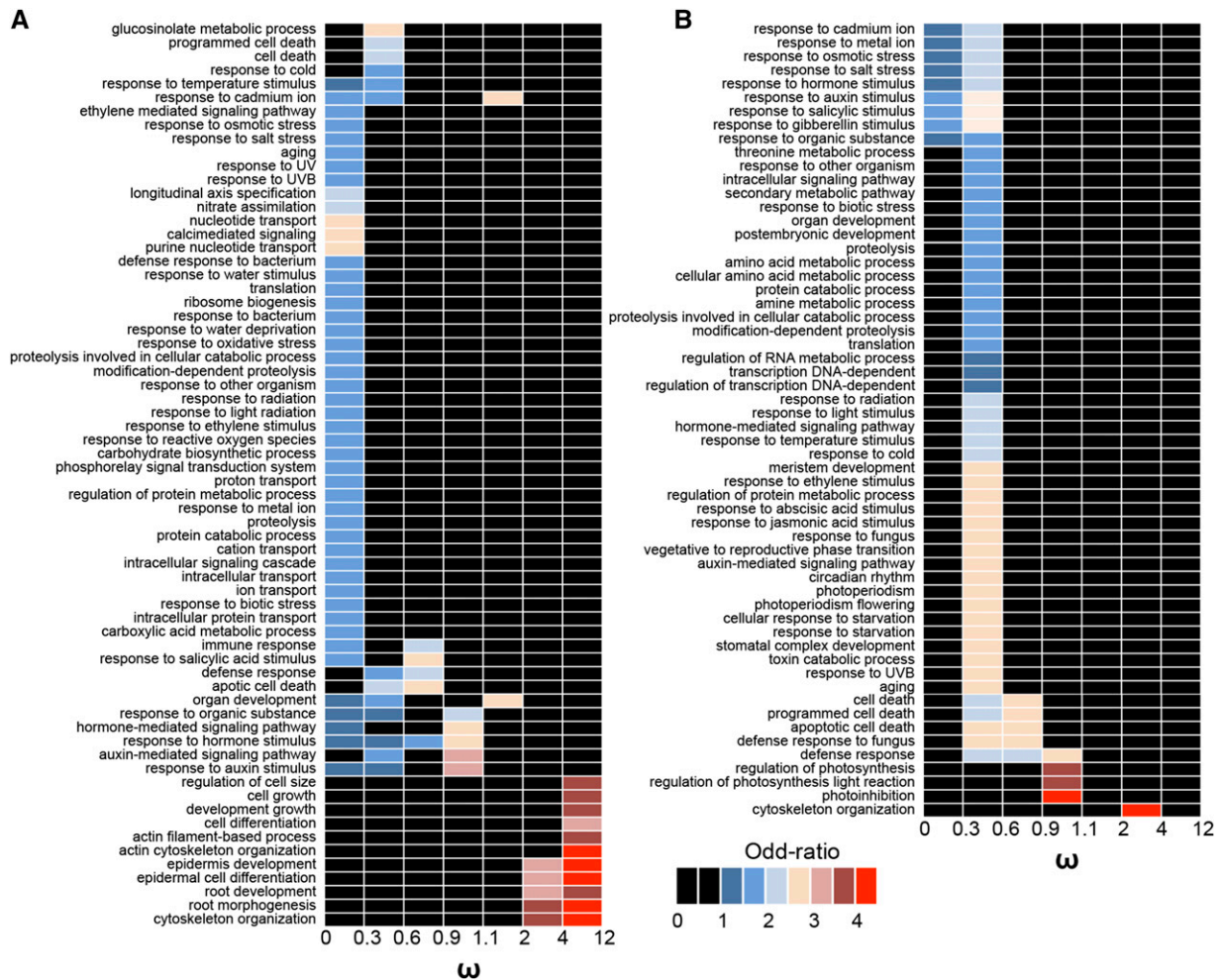


**Figure 4.** Overrepresented GO Categories of  $\alpha$ -Duplicates and BI-m-Duplicates Retained under Different Selection Regimes in Buckler Mustard.

$\alpha$ -Duplicates (**A**) and BI-m-duplicates (**B**). The strength of selection between duplicates is considered according to  $\omega$  (i.e.,  $K_a/K_s$  ratio): strong purifying selection ( $\omega < 0.6$ ) versus weak selection or neutral divergence ( $\omega$  between 0.6 and 2) versus strong positive selection ( $\omega > 2$ ). Significantly overrepresented categories are shown by colors according to the panel and corresponding to odd ratios quantifying the enrichment of the particular GO term (i.e., effect size), whereas categories in black are not significant at corrected  $\alpha = 0.05$ .

Schemske, 2002), to what extent adaptive diversification of cytoskeleton genes may support the necessary scaling of intracellular structures after WGDs should be further examined (Hazel et al., 2013).

The vast majority of retained duplicates in *B. laevigata* presented evidence of purifying selection, matching the hypothesis that dosage effects are crucial in maintaining functional traits after WGDs (Birchler and Veitia, 2012). In the absence of a complete atlas of transcripts coupled with a high-quality genome sequence, only partial conclusions can be drawn. In particular, that specific duplicates have evolved partially different functions is not excluded, but high-quality GO annotations from Arabidopsis are expected to provide reliable insights in this non-model relative (Primmer et al., 2013). Remarkably, the relatively young BI-m-duplicates with evidence of strong purifying selection were specifically enriched in functional categories related to stressing environments. Despite offering only candidate genes and genetic

pathways of adaptive significance, such quantitative inference strongly supports that environmental constraints played an influential role in shaping genome fractionation in Buckler mustard. Accordingly, ploidy-dependent uptake of soil minerals and tolerance to salinity has recently been demonstrated (Chao et al., 2013). Here, a majority of the BI-m-duplicates involved in responses to soil chemistry showed evidence of purifying selection, indicating that increased dosage may have enhanced tolerance of *Biscutella* to stressing edaphic conditions (Veitia et al., 2013), which is coherent with the species adaptation to toxic soils such as found on serpentine or mines (Gasser, 1986; Babst-Kostecka et al., 2014, and references therein). Several of the retained duplicates involved in responses to light and temperatures show a similar pattern and also represent strong candidates having been adaptively recruited during radiation of Buckler mustard across alpine habitats (Körner, 2003). Shifts from Mediterranean to alpine environments have indeed been postulated for several polyploid

species (Favarger, 1971), matching the observed rounds of WGD fractionation in Buckler mustard. The underpinnings of the colonization of new environments remain elusive, but available insights suggest that adaptive retention of extra doses of functional duplicates likely supported establishment into otherwise harsh conditions. This hypothesis remains largely to be tested.

### Cycles of WGD: Fractionation

Fractionation in Buckler mustard resulted in the retention of large chromosome segments interrupted by GB sections presenting decay of fluorescence (Figure 3). Molecular mechanisms driving such uneven genome reorganization are unknown, but likely involved DNA loss and dynamics of transposable elements such as regularly reported in this and other polyploids (Freeling et al., 2012; Woodhouse et al., 2014; Bardil et al., 2015). Recurrent WGD fractionation cycles point here to a balance between conservation of specific loci and high sequence turnover across other regions, matching predictions of Conant et al. (2014) that duplicates are initially preserved under purifying selection before some duplicates accumulate mutations leading to functional changes to be recruited under positive selection. The surmised impact of environmental constraints in shaping fractionation after the breaking of genetic constraints by WGD likely explains patterns of polyploid radiation and calls for additional studies addressing the contribution of ecological stresses during genome evolution (Wagner, 2011; Nei, 2013).

## METHODS

### Plant Materials and Cultivation Conditions

Four individuals of *Biscutella laevigata* subsp *laevigata* ( $2n = 4x = 36$ ) were collected in a previously described population (Parisod and Christin, 2008), grown outdoors for 1 year in a common garden (Botanical Garden of Neuchâtel, Switzerland), and analyzed there.

### CCP

Whole inflorescences from individuals of *B. laevigata* subsp *varia* ( $2n = 2x = 18$ ), used by Bardil et al. (2015), were fixed in freshly prepared ethanol:acetic acid fixative (3:1) overnight, transferred into 70% ethanol, and stored at  $-20^{\circ}\text{C}$  until use. Selected inflorescences were rinsed in distilled water and citrate buffer (10 mM sodium citrate, pH 4.8) and digested in a 0.3% mix of pectolytic enzymes (cellulase, cytohelicase, and pectolyase; all from Sigma-Aldrich) in citrate buffer for  $\sim 3$  h. Individual anthers were disintegrated on a microscopic slide by a needle in a drop of water. The suspension was then softened by adding 20  $\mu\text{L}$  of 60% acetic acid, spread by stirring with a needle on a hot plate at  $50^{\circ}\text{C}$  for 2 min, fixed by adding 100  $\mu\text{L}$  of ethanol:acetic acid fixative (3:1), postfixed in 4% formaldehyde in water (10 min), and air-dried. Chromosome preparations were pretreated with RNase (100  $\mu\text{g}/\text{mL}$ ; AppliChem) and pepsin (0.1 mg/mL; Sigma-Aldrich) dissolved in 0.01 M HCl for 10 min, postfixed in 4% formaldehyde in  $2\times$  SSC ( $2\times$  SSC is 3M sodium chloride and 300 mM trisodium citrate, pH 7.0) for 10 min, and dehydrated in an ethanol series (70, 80, and 96%).

The BAC clone T15P10 (AF167571) bearing 35S rRNA genes was used for in situ localization of 35S rDNA, and the clone pCT 4.2 corresponding to 500-bp 5S rRNA repeat (M65137) was used for localization of 5S rDNA loci. For CCP, a total of 547 *Arabidopsis thaliana* BAC clones were assembled to represent the 24 GBs of the ancestral crucifer karyotype (Schranz et al., 2006; Supplemental Table 4). To further characterize the orientation and

internal structure of particular GBs, the respective BAC contigs were arbitrarily broken into smaller subcontigs and differentially labeled. DNA probes were labeled with biotin-dUTP, digoxigenin-dUTP, or Cy3-dUTP by nick translation as described by Mandáková et al. (2010). Labeled BAC DNAs were pooled, precipitated, and resuspended in 20  $\mu\text{L}$  of hybridization mixture (50% formamide and 10% dextran sulfate in  $2\times$  SSC) per slide. Labeled probes and chromosomes were denatured together on a hot plate at  $80^{\circ}\text{C}$  for 2 min and incubated in a moist chamber at  $37^{\circ}\text{C}$  for 16 to 72 h. Posthybridization washing was performed in 20% formamide in  $2\times$  SSC at  $42^{\circ}\text{C}$ . Immunodetection was performed as follows: biotin-dUTP was detected by avidin-Texas Red (Vector Laboratories) and signals amplified by goat anti-avidin-biotin (Vector Laboratories) and avidin-Texas Red; digoxigenin-dUTP was detected by mouse antidigoxigenin (Jackson ImmunoResearch) and goat anti-mouse-Alexa Fluor 488 (Molecular Probes). Cy3-dUTP-labeled probes were observed directly. Chromosomes were counterstained by 4',6-diamidino-2-phenylindole (2  $\mu\text{g}/\text{mL}$ ) in Vectashield (Vector Laboratories). Fluorescence signals were analyzed with an Olympus BX-61 epifluorescence microscope and CoolCube CCD camera (MetaSystems). Images were acquired separately for the four fluorochromes using appropriate excitation and emission filters (AHF Analytentechnik). The four monochromatic images were pseudocolored and merged using Adobe Photoshop CS2 software (Adobe Systems).

The length and fluorescence intensity of selected GBs were measured on average in 10 pachytene chromosomes using Image J software (National Institutes of Health). For determining the level of fluorescence, corrected total fluorescence (Burgess et al., 2010; Potapova et al., 2011) was calculated: corrected total fluorescence = integrated density – (area of selected chromosome segment  $\times$  mean fluorescence of background readings). BAC painted chromosomes in Figure 3 were straightened using the plug-in “Straighten Curved Objects” (Kocsis et al., 1991) in Image J with sub-blocks differentially labeled according to Supplemental Data Set 1.

### cDNA Library Preparation and Transcriptome Sequencing

Tissue from young leaves and roots of the four individuals of *B. laevigata* subsp *laevigata* ( $2n = 4x = 36$ ) were simultaneously collected in liquid nitrogen, and total RNA was extracted using PureLink RNA Mini Kit (Life Technologies), following the manufacturer's instructions. RNA quality was checked with the Agilent bioanalyzer. A 454 normalized library was prepared on poly(A)-enriched RNAs from root and leaf tissues of one individual that were pooled, fragmented, and single-end sequenced on a quarter of a plate using Roche GS FLX Titanium Series (service provided by Microsynth, following the manufacturer's instructions). Six quantitative cDNA libraries (four individuals; two with pooled root and leaf; two with root and leaf separated; Supplemental Table 1) were prepared and bar-coded for SOLiD, mixed, and single-end sequenced on six lanes of SOLiD 5500xl (service provided by Microsynth, following the manufacturer's instructions).

### Transcriptome Assembly and Annotation

After trimming of adaptor sequences, reads of low quality or showing GC bias and reads of low complexity or size as well as exact duplicates were removed using PRINSEQ (Schmieder and Edwards, 2011) and FASTX-Toolkit ([http://hannonlab.cshl.edu/fastx\\_toolkit/](http://hannonlab.cshl.edu/fastx_toolkit/)).

Transcriptome assembly was performed through six iterative steps using the hybrid mode of MIRA (Chevreux et al., 2004). As a first step, 454 reads were assembled with a SOLiD library to obtain a first set of assembled contigs as well as singletons. Contigs were then used together with the 454 library in a new round of hybrid assembly with a new SOLiD library. Previously assembled contigs that failed to be elongated at this specific step were retrieved from singletons and merged back with contigs for further elongation in a new round of hybrid assembly. This iterative procedure was



followed until all SOLID libraries were included. At each step, summary statistics were computed on the resulting set of contigs to follow improvement of the assembly (Supplemental Table 2). At the final step, singletons and exact duplicates as well as contigs shorter than 150 bp were filtered out to produce the working set of transcripts (i.e., transcriptome).

BLAST against various databases (e.g., nucleotide collection of NCBI) returned hits from various Brassicaceae for the vast majority of assembled contigs (data not shown). We decided to rely on the TAIR10 database and its accurate annotations from Arabidopsis (Lamesch et al., 2012) for subsequent analyses (Primmer et al., 2013). Assembled contigs were annotated by BLASTx (minimum e-values set at e-5 and e-10) against the TAIR 10 peptide database. Reading frames were identified and excised through comparison with the TAIR10 database using Exonerate (Slater and Birney, 2005).

Assuming that gene order within BACs is conserved between Arabidopsis and *Biscutella*, unigenes were assigned to GBs (Supplemental Table 4) according to their annotation (Schranz et al., 2006). Transcript coverage along GBs was then assessed using overlapping sliding windows of 40 loci from the Arabidopsis reference genome (increment of 10), visualizing the representativeness of the *B. laevigata* transcriptome. The distribution of retained duplicates along GBs was similarly assessed as the proportion of loci with transcripts showing evidence of BI-m-duplicates. Coordinates of BAC clones used for GB painting (Supplemental Data Set 1) were used to determine encompassed genes and collocate transcriptome and cytogenetic data.

### Inference of WGD from Transcriptome

After having filtered out mitochondrial and plastid genes as well as transposable element containing genes, framed contigs showing higher than 30% sequence similarity over at least 450 bp were grouped into gene families (custom script). Transcripts from clusters with at least two members were aligned using the codon-aware MACSE algorithm (Ranwez et al., 2011). Corresponding phylogenetic trees were inferred with FastTree (Price et al., 2009) to infer synonymous and nonsynonymous substitutions ( $K_s$  and  $K_a$ , respectively) in PAML using the F3X4 model (Yang, 2007).

The fixation rate of synonymous substitutions being relatively constant,  $K_s$  can be used to evaluate the time of duplication between two sequences (Maere et al., 2005). When all genes are duplicated simultaneously during WGD, the  $K_s$  distribution of resulting pairs of transcripts is approximately Gaussian (Blanc and Wolfe, 2004). Accordingly, mixture models can infer WGD events by fitting normal distributions to the data (Barker et al., 2009). After removal of identical pairs of contigs (i.e.,  $K_s = 0$ ) as well as pairs with  $K_s > 2$  that proved less reliable for inference of WGDs (Vanneste et al., 2013), normal peaks in the distribution of  $K_s$  between members of gene families were accordingly inferred using the package mixtools in R cran (Benaglia et al., 2009). Both  $K_s$  and root-squared  $K_s$  values were analyzed and gave similar results. The most likely number of normal distributions in the observed distribution of  $K_s$  among pairs of transcripts was tested by a parametric bootstrap analysis (100 bootstraps) comparing the likelihood ratio of  $k$  versus  $k + 1$  in between  $k = 1$  and  $k = 10$ . Then, the iterative “expectation-maximization” algorithm (i.e., normalmixEM procedure) converged to the positions and standard deviations of four normal distributions that were further evaluated by 100 bootstraps.

Converting  $K_s$  time equivalents into real time using the  $\alpha$ -WGD event (mean  $K_s = 0.896$ ) as a calibration point offered rough estimates of the time of duplication events. Following Hohmann et al. (2015), we used 32.42 million years as the minimum age of  $\alpha$ -WGD event (Lysak and Koch, 2011). A constant accumulation of synonymous mutations among simultaneously duplicated transcripts with  $K_s < 2$  was assumed and used to scale the mean  $K_s$  and  $sd$  of normal peaks into time since WGD events.

### Biased Retention of Duplicated Transcripts

Overrepresented GO categories among framed contigs larger than 150 bp that were not grouped in gene families compared with those having been

included in a group (i.e., retained duplicates) was assessed using FatiGo (Al-Shahrour et al., 2004).

Duplicated pairs of transcripts (i.e., contigs grouped in a family) were assigned to their WGD event of origin according to their  $K_s$  value caught between the 5% and the 95% quantiles of the corresponding peak. For the  $\alpha$ -WGD event (mean  $K_s = 0.896$ ), this interval was artificially truncated to  $\alpha$ -duplicates with  $K_s$  ranging from 0.41 to 0.90, avoiding possible inclusion of duplicates from the  $\beta$ -WGD event. For the BI-m-WGD event (mean  $K_s = 0.235$ ), duplicates with  $K_s$  ranging from 0.085 to 0.37 were considered as BI-m-duplicates. Difference in the proportion of retained duplicates after the  $\alpha$ - versus BI-m-WGD events was assessed with a two-sided non-parametric proportion test and evolutionary forces underlying their retention were inferred by computing their  $K_a/K_s$  ratios (i.e.,  $\omega$ ) using PAML (Yang, 2007). The proportion of retained duplicates after the BI-m-WGD event was associated with ratio of the physical length and painting intensity between duplicated GBs A, B, E, J, O, P, R, and U, using robust regressions (FastLTS approach) with P values assessed through permutation.

Using high-quality annotations of unigenes from the Arabidopsis reference, overrepresented GO categories of duplicated transcripts showing evidence purifying selection (i.e.,  $\omega$  below 0.9: strong from 0 to 0.6 or weak from 0.6 to 0.9), neutral divergence (i.e.,  $\omega$  of 0.9 to 1.1), or positive selection (i.e.,  $\omega$  higher than 1: weak from 1.1 to 2, strong from 2 to 12) compared with the whole transcriptome data set were assessed separately using FatiGo (Al-Shahrour et al., 2004). Significance was assessed according to Fisher's exact tests and adjusted P values corrected for multiple testing with the false discovery rate procedure (Benjamini and Hochberg, 1995). Odds ratio, quantifying the probability that the list is enriched in a particular term, further provided insights on the strength of the association (i.e., effect size). Significantly overexpressed GO terms at the 0.05 level were retrieved and summarized by their GO classification (<ftp://ftp.arabidopsis.org>).

### Accession Numbers

Sequence data and the assembled transcriptome are under the GenBank BioProject PRJNA302858.

### Supplemental Data

**Supplemental Figure 1.** Scenario of genome evolution in *Biscutella* from the ancestral crucifer karyotype.

**Supplemental Figure 2.** Transcriptome data along each genomic block.

**Supplemental Figure 3.** Distribution of synonymous substitutions between pairs of duplicated transcripts.

**Supplemental Table 1.** Sequenced cDNA libraries.

**Supplemental Table 2.** Iterative hybrid assembly of cDNA libraries.

**Supplemental Table 3.** Overall retention bias of transcripts.

**Supplemental Table 4.** Genomic blocks of the ancestral crucifer karyotype.

**Supplemental Analysis.** Phylogenetics of gene pairs under whole-genome duplications.

**Supplemental Data Set 1.** Genomic sub-blocks used for fine-scale comparative chromosome painting.

### ACKNOWLEDGMENTS

We thank two anonymous reviewers for valuable comments on a previous draft of the manuscript and S. Zoller and A. Bardil for their help with bioinformatic analyses. Analyses were performed using facilities of the

Genetic Diversity Centre, ETH Zurich. N.A. is funded by a grant from the Swiss National Science Foundation. Work in the Lysak lab was supported by the Czech Science Foundation (Grant 13-10159S) and by the European Social Fund (Projects CZ.1.07/2.3.00/30.0037 and CZ.1.07/2.3.00/20.0189). Work in the Parisod lab was supported by the Velux Stiftung (Project 705) and the Swiss National Science Foundation (Grant PZ00P3-131950).

#### AUTHOR CONTRIBUTIONS

C.G. and C.P. completed the transcriptome assembly, analysis, and interpretation, with assistance from N.A. T.M. and M.A.L. completed and interpreted the cytogenetics work. C.P. and T.M. integrated transcriptome and cytogenetics data. C.G., M.A.L., and C.P. wrote the manuscript. All authors commented and approved the final manuscript.

Received September 10, 2015; revised December 2, 2015; accepted December 10, 2015; published December 14, 2015.

#### REFERENCES

- Al-Shahrour, F., Díaz-Uriarte, R., and Dopazo, J.** (2004). Fatigo: a web tool for finding significant associations of Gene Ontology terms with groups of genes. *Bioinformatics* **20**: 578–580.
- Arrigo, N., and Barker, M.S.** (2012). Rarely successful polyploids and their legacy in plant genomes. *Curr. Opin. Plant Biol.* **15**: 140–146.
- Babst-Kostecka, A.A., Parisod, C., Godé, C., Vollenweider, P., and Pauwels, M.** (2014). Patterns of genetic divergence among populations of the pseudometallophyte *Biscutella laevigata* from southern Poland. *Plant Soil* **383**: 245–256.
- Bardil, A., Tayalé, A., and Parisod, C.** (2015). Evolutionary dynamics of retrotransposons following autopolyploidy in the Buckler Mustard species complex. *Plant J.* **82**: 621–631.
- Barker, M.S., Vogel, H., and Schranz, M.E.** (2009). Paleopolyploidy in the Brassicales: analyses of the Cleome transcriptome elucidate the history of genome duplications in Arabidopsis and other Brassicales. *Genome Biol. Evol.* **1**: 391–399.
- Benaglia, T., Chauveau, D., Hunter, D.R., and Young, D.S.** (2009). mixtools: An R package for analyzing finite mixture models. *J. Stat. Softw.* **32**: 1–29.
- Benjamini, Y., and Hochberg, Y.** (1995). Controlling the false discovery rate - a practical and powerful approach to multiple testing. *J. R. Stat. Soc. B* **57**: 289–300.
- Birchler, J.A., and Veitia, R.A.** (2012). Gene balance hypothesis: connecting issues of dosage sensitivity across biological disciplines. *Proc. Natl. Acad. Sci. USA* **109**: 14746–14753.
- Blanc, G., and Wolfe, K.H.** (2004). Widespread paleopolyploidy in model plant species inferred from age distributions of duplicate genes. *Plant Cell* **16**: 1667–1678.
- Blondel, J., Aronson, J., Bodiou, J.-Y., and Boeuf, G.** (2010). The Mediterranean Region: Biological Diversity in Space and Time. (Oxford, UK: Oxford University Press).
- Bowers, J.E., Chapman, B.A., Rong, J., and Paterson, A.H.** (2003). Unravelling angiosperm genome evolution by phylogenetic analysis of chromosomal duplication events. *Nature* **422**: 433–438.
- Burgess, A., Vigneron, S., Brioude, E., Labbé, J.-C., Lorca, T., and Castro, A.** (2010). Loss of human Greatwall results in G2 arrest and multiple mitotic defects due to deregulation of the cyclin B-Cdc2/PP2A balance. *Proc. Natl. Acad. Sci. USA* **107**: 12564–12569.
- Chalhoub, B., et al.** (2014). Plant genetics. Early allopolyploid evolution in the post-Neolithic *Brassica napus* oilseed genome. *Science* **345**: 950–953.
- Chao, D.-Y., Dilkes, B., Luo, H., Douglas, A., Yakubova, E., Lahner, B., and Salt, D.E.** (2013). Polyploids exhibit higher potassium uptake and salinity tolerance in *Arabidopsis*. *Science* **341**: 658–659.
- Chevreux, B., Pfisterer, T., Drescher, B., Driesel, A.J., Müller, W.E.G., Wetter, T., and Suhai, S.** (2004). Using the miraEST assembler for reliable and automated mRNA transcript assembly and SNP detection in sequenced ESTs. *Genome Res.* **14**: 1147–1159.
- Conant, G.C., Birchler, J.A., and Pires, J.C.** (2014). Dosage, duplication, and diploidization: clarifying the interplay of multiple models for duplicate gene evolution over time. *Curr. Opin. Plant Biol.* **19**: 91–98.
- Couvreur, T.L.P., Franzke, A., Al-Shehbaz, I.A., Bakker, F.T., Koch, M.A., and Mummenhoff, K.** (2010). Molecular phylogenetics, temporal diversification, and principles of evolution in the mustard family (Brassicaceae). *Mol. Biol. Evol.* **27**: 55–71.
- De Smet, R., Adams, K.L., Vandepoele, K., Van Montagu, M.C.E., Maere, S., and Van de Peer, Y.** (2013). Convergent gene loss following gene and genome duplications creates single-copy families in flowering plants. *Proc. Natl. Acad. Sci. USA* **110**: 2898–2903.
- Doyle, J.J., Flagel, L.E., Paterson, A.H., Rapp, R.A., Soltis, D.E., Soltis, P.S., and Wendel, J.F.** (2008). Evolutionary genetics of genome merger and doubling in plants. *Annu. Rev. Genet.* **42**: 443–461.
- Edger, P.P., et al.** (2015). The butterfly plant arms-race escalated by gene and genome duplications. *Proc. Natl. Acad. Sci. USA* **112**: 8362–8366.
- Favarger, C.** (1971). Relations entre la flore méditerranéenne et celle des enclaves à végétation subméditerranéenne d'Europe centrale. *Boissiera* **19**: 149–168.
- Fawcett, J.A., Maere, S., and Van de Peer, Y.** (2009). Plants with double genomes might have had a better chance to survive the Cretaceous-Tertiary extinction event. *Proc. Natl. Acad. Sci. USA* **106**: 5737–5742.
- Flagel, L.E., and Wendel, J.F.** (2009). Gene duplication and evolutionary novelty in plants. *New Phytol.* **183**: 557–564.
- Freeling, M.** (2009). Bias in plant gene content following different sorts of duplication: tandem, whole-genome, segmental, or by transposition. *Annu. Rev. Plant Biol.* **60**: 433–453.
- Freeling, M., Woodhouse, M.R., Subramaniam, S., Turco, G., Lisch, D., and Schnable, J.C.** (2012). Fractionation mutagenesis and similar consequences of mechanisms removing dispensable or less-expressed DNA in plants. *Curr. Opin. Plant Biol.* **15**: 131–139.
- Garsmeur, O., Schnable, J.C., Almeida, A., Jourda, C., D'Hont, A., and Freeling, M.** (2014). Two evolutionarily distinct classes of paleopolyploidy. *Mol. Biol. Evol.* **31**: 448–454.
- Gasser, M.** (1986). Genetic-ecological investigations in *Biscutella laevigata* L. *Veröff. Geobot. Inst. ETH.* **86**: 7–86.
- Hazel, J., Krutkramelis, K., Mooney, P., Tomschik, M., Gerow, K., Oakey, J., and Gatlin, J.C.** (2013). Changes in cytoplasmic volume are sufficient to drive spindle scaling. *Science* **342**: 853–856.
- Hohmann, N., Wolf, E.M., Lysak, M.A., and Koch, M.A.** (2015). A time-calibrated road map of Brassicaceae species radiation and evolutionary history. *Plant Cell* **27**: 2770–2784.
- Innan, H., and Kondrashov, F.** (2010). The evolution of gene duplications: classifying and distinguishing between models. *Nat. Rev. Genet.* **11**: 97–108.
- Jalas, J., Suominen, J., and Lampinen, R.** (1996). *Atlas Florae Europaeae*. (Helsinki, Finland: The Academic Bookstore).
- Jiao, Y., et al.** (2011). Ancestral polyploidy in seed plants and angiosperms. *Nature* **473**: 97–100.
- Kagale, S., Robinson, S.J., Nixon, J., Xiao, R., Huebert, T., Condie, J., Kessler, D., Clarke, W.E., Edger, P.P., Links, M.G., Sharpe, A.G., and Parkin, I.A.P.** (2014). Polyploid evolution of the Brassicaceae during the Cenozoic era. *Plant Cell* **26**: 2777–2791.
- Kocsis, E., Trus, B.L., Steer, C.J., Bisher, M.E., and Steven, A.C.** (1991). Image averaging of flexible fibrous macromolecules: the clathrin triskelion has an elastic proximal segment. *J. Struct. Biol.* **107**: 6–14.

- Körner, C.** (2003). *Alpine Plant Life*. (Heidelberg, Germany: Springer Verlag).
- Lamesch, P., et al.** (2012). The Arabidopsis Information Resource (TAIR): improved gene annotation and new tools. *Nucleic Acids Res.* **40**: D1202–D1210.
- Lim, K.Y., Kovarik, A., Matyasek, R., Chase, M.W., Clarkson, J.J., Grandbastien, M.A., and Leitch, A.R.** (2007). Sequence of events leading to near-complete genome turnover in allopolyploid *Nicotiana* within five million years. *New Phytol.* **175**: 756–763.
- Lynch, M., and Conery, J.S.** (2000). The evolutionary fate and consequences of duplicate genes. *Science* **290**: 1151–1155.
- Lysak, M.A., and Koch, M.A.** (2011). Phylogeny, genome, and karyotype evolution of Crucifers (Brassicaceae). In *Genetics and Genomics of the Brassicaceae*, R. Schmidt and I. Bancroft, eds (New York: Springer-Verlag), pp. 1–31.
- Maere, S., De Bodt, S., Raes, J., Casneuf, T., Van Montagu, M., Kuiper, M., and Van de Peer, Y.** (2005). Modeling gene and genome duplications in eukaryotes. *Proc. Natl. Acad. Sci. USA* **102**: 5454–5459.
- Mandáková, T., Joly, S., Krzywinski, M., Mummenhoff, K., and Lysak, M.A.** (2010). Fast diploidization in close mesopolyploid relatives of *Arabidopsis*. *Plant Cell* **22**: 2277–2290.
- Mandáková, T., and Lysak, M.A.** (2008). Chromosomal phylogeny and karyotype evolution in  $x=7$  crucifer species (Brassicaceae). *Plant Cell* **20**: 2559–2570.
- Manton, I.** (1937). The problem of *Biscutella laevigata* L. II. The evidence from meiosis. *Ann. Bot. (Lond.)* **51**: 439–465.
- McGrath, C.L., and Lynch, M.** (2012). Evolutionary significance of whole-genome duplication. In *Polyploidy and Genome Evolution*, P.S. Soltis and D.E. Soltis, eds (Berlin, Heidelberg, Germany: Springer-Verlag), pp. 1–20.
- Nei, M.** (2013). *Mutation-Driven Evolution*. (Oxford, UK: Oxford University Press).
- Ohno, S.** (1970). *Evolution by Gene Duplication*. (Berlin, Germany: Springer).
- Olowokudejo, J.D.** (1986). The infrageneric classification of *Biscutella* (Cruciferae). *Brittonia* **38**: 86–88.
- Parisod, C., and Besnard, G.** (2007). Glacial in situ survival in the Western Alps and polytopic autopolyploidy in *Biscutella laevigata* L. (Brassicaceae). *Mol. Ecol.* **16**: 2755–2767.
- Parisod, C., and Christin, P.A.** (2008). Genome-wide association to fine-scale ecological heterogeneity within a continuous population of *Biscutella laevigata* (Brassicaceae). *New Phytol.* **178**: 436–447.
- Parisod, C., Holderegger, R., and Brochmann, C.** (2010). Evolutionary consequences of autopolyploidy. *New Phytol.* **186**: 5–17.
- Potapova, T.A., Sivakumar, S., Flynn, J.N., Li, R., and Gorbsky, G.J.** (2011). Mitotic progression becomes irreversible in prometaphase and collapses when Wee1 and Cdc25 are inhibited. *Mol. Biol. Cell* **22**: 1191–1206.
- Price, M.N., Dehal, P.S., and Arkin, A.P.** (2009). FastTree: computing large minimum evolution trees with profiles instead of a distance matrix. *Mol. Biol. Evol.* **26**: 1641–1650.
- Primmer, C.R., Papakostas, S., Leder, E.H., Davis, M.J., and Ragan, M.A.** (2013). Annotated genes and nonannotated genomes: cross-species use of Gene Ontology in ecology and evolutionary research. *Mol. Ecol.* **22**: 3216–3241.
- Ramsey, J., and Schemske, D.W.** (2002). Neopolyploidy in flowering plants. *Annu. Rev. Ecol. Syst.* **33**: 589–639.
- Ranwez, V., Harispe, S., Delsuc, F., and Douzery, E.J.P.** (2011). MACSE: Multiple Alignment of Coding SEquences accounting for frameshifts and stop codons. *PLoS One* **6**: e22594.
- Schmieder, R., and Edwards, R.** (2011). Quality control and preprocessing of metagenomic datasets. *Bioinformatics* **27**: 863–864.
- Schönfelder, P.** (1968). Chromozomenzahlen einiger Arten der Gattung *Biscutella* L. *Österreichische Botanische Zeitschrift* **115**: 363–371.
- Schranz, M.E., Lysak, M.A., and Mitchell-Olds, T.** (2006). The ABC's of comparative genomics in the Brassicaceae: building blocks of crucifer genomes. *Trends Plant Sci.* **11**: 535–542.
- Schranz, M.E., Mohammadin, S., and Edger, P.P.** (2012). Ancient whole genome duplications, novelty and diversification: the WGD Radiation Lag-Time Model. *Curr. Opin. Plant Biol.* **15**: 147–153.
- Slater, G.S., and Birney, E.** (2005). Automated generation of heuristics for biological sequence comparison. *BMC Bioinformatics* **6**: 31.
- Soltis, D.E., Segovia-Salcedo, M.C., Jordon-Thaden, I., Majure, L., Miles, N.M., Mavrodiev, E.V., Mei, W., Cortez, M.B., Soltis, P.S., and Gitzendanner, M.A.** (2014). Are polyploids really evolutionary dead-ends (again)? A critical reappraisal of Mayrose et al. (). *New Phytol.* **202**: 1105–1117.
- Tang, H., Woodhouse, M.R., Cheng, F., Schnable, J.C., Pedersen, B.S., Conant, G., Wang, X., Freeling, M., and Pires, J.C.** (2012). Altered patterns of fractionation and exon deletions in *Brassica rapa* support a two-step model of paleohexaploidy. *Genetics* **190**: 1563–1574.
- Tank, D.C., Eastman, J.M., Pennell, M.W., Soltis, P.S., Soltis, D.E., Hinchliff, C.E., Brown, J.W., Sessa, E.B., and Harmon, L.J.** (2015). Nested radiations and the pulse of angiosperm diversification: increased diversification rates often follow whole genome duplications. *New Phytol.* **207**: 454–467.
- Tayalé, A., and Parisod, C.** (2013). Natural pathways to polyploidy in plants and consequences for genome reorganization. *Cytogenet. Genome Res.* **140**: 79–96.
- Tremetsberger, K., König, C., Samuel, R., Pinsker, W., and Stuessy, T.F.** (2002). Intraspecific genetic variation in *Biscutella laevigata* (Brassicaceae): new focus on Irene Manton's hypothesis. *Plant Syst. Evol.* **233**: 163–181.
- Van de Peer, Y., Maere, S., and Meyer, A.** (2009). The evolutionary significance of ancient genome duplications. *Nat. Rev. Genet.* **10**: 725–732.
- Vanneste, K., Baele, G., Maere, S., and Van de Peer, Y.** (2014b). Analysis of 41 plant genomes supports a wave of successful genome duplications in association with the Cretaceous-Paleogene boundary. *Genome Res.* **24**: 1334–1347.
- Vanneste, K., Maere, S., and Van de Peer, Y.** (2014a). Tangled up in two: a burst of genome duplications at the end of the Cretaceous and the consequences for plant evolution. *Philos. Trans. R. Soc. Lond. B Biol. Sci.* **369**: 20130353.
- Vanneste, K., Van de Peer, Y., and Maere, S.** (2013). Inference of genome duplications from age distributions revisited. *Mol. Biol. Evol.* **30**: 177–190.
- Veitia, R.A., Bottani, S., and Birchler, J.A.** (2013). Gene dosage effects: nonlinearities, genetic interactions, and dosage compensation. *Trends Genet.* **29**: 385–393.
- Wagner, A.** (2011). *The Origins of Evolutionary Innovations*. (Oxford, UK: Oxford University Press).
- Wolfe, K.H.** (2001). Yesterday's polyploids and the mystery of diploidization. *Nat. Rev. Genet.* **2**: 333–341.
- Wood, T.E., Takebayashi, N., Barker, M.S., Mayrose, I., Greenspoon, P.B., and Rieseberg, L.H.** (2009). The frequency of polyploid speciation in vascular plants. *Proc. Natl. Acad. Sci. USA* **106**: 13875–13879.
- Woodhouse, M.R., Cheng, F., Pires, J.C., Lisch, D., Freeling, M., and Wang, X.** (2014). Origin, inheritance, and gene regulatory consequences of genome dominance in polyploids. *Proc. Natl. Acad. Sci. USA* **111**: 5283–5288.
- Yang, Z.** (2007). PAML 4: phylogenetic analysis by maximum likelihood. *Mol. Biol. Evol.* **24**: 1586–1591.